J Nanopart Res (2014) 16:2621
DOI 10.1007/s11051-014-2621-x

RESEARCH PAPER

Biocompatible hyaluronic acid polymer-coated quantum dots for CD44$^+$ cancer cell-targeted imaging

Hening Wang · Hongfang Sun · Hui Wei · Peng Xi · Shuming Nie · Qiushi Ren

Received: 10 June 2014 / Accepted: 21 August 2014

Abstract The cysteamine-modified hyaluronic acid (HA) polymer was employed to coat quantum dots (QDs) through a convenient one-step reverse micelle method, with the final QDs hydrodynamic size of around 22.6 nm. The HA coating renders the QDs with very good stability in PBS for more than 140 days and resistant to large pH range of 2–12. Besides, the HA-coated QDs also show excellent fluorescence stability in BSA-containing cell culture medium. In addition, the cell culture assay indicates no significant cytotoxicity for MD-MB-231 breast cancer cells, and its targeting ability to cancer receptor CD44 has been demonstrated on two breast cancer cell lines. The targeting mechanism was further proved by the HA competition experiment. This work has established a new approach to help solve the stability and toxicity problems of QDs, and moreover render the QDs cancer targeting property. The current results indicate that the HA polymer-coated QDs hold the potential application for both in vitro and in vivo cancer imaging researches.

Keywords Quantum dots · Hyaluronic acid · Biocompatibility · CD44 receptor · Molecular imaging · Nanomedicine

H. Wang · H. Sun · P. Xi · Q. Ren (✉)
Department of Biomedical Engineering, Peking University, No.5 Yiheyuan Road, Haidian District, Beijing 100871, People's Republic of China
e-mail: renqsh@coe.pku.edu.cn

H. Wang · H. Wei · S. Nie (✉)
Department of Biomedical Engineering, Emory University and Georgia Institute of Technology, 1760 Haygood Drive, Room E116, Atlanta, GA 30322, USA
e-mail: snie@emory.edu

Introduction

Semiconductor quantum dots (QDs) have been widely used for biomedical applications due to their unique optical and electronic properties (Bruchez et al. 1998; Chan et al. 2002; Chan and Nie 1998; Cheng et al. 2014; Gao et al. 2004; Medintz et al. 2005; Ruan et al. 2007; Smith et al. 2008a; Steponkiene et al. 2014; Wu et al. 2002; Xing et al. 2007; Zheng et al. 2010). Compared with traditional organic dyes and fluorescent proteins, QDs are highly bright and resistant to photo-bleaching. Even importantly they have size, composition, and lattice strain tunable emission wavelength (Leutwyler et al. 1996; Smith et al. 2008a, b; Smith and Nie 2011). However, great concern has been raised over the application of quantum dots in living cells and animals due to their chemical composition of toxic heavy metals like Cd. Some studies have indicated that the cytotoxicity of QDs strongly correlated with the stability and surface coatings of these nanoparticles (Derfus et al. 2004; Gao et al. 2004; Hu and Gao 2010; Wu et al. 2002).

Published online: 19 September 2014

Besides, for biomedical applications, ideal QDs should not only have good water solubility, high stability, minimized cell toxicity, but also have abundant functional groups such as amine ($–NH_2$) and carboxyl (–COOH) groups for further conjugation toward specific targeted imaging.

Because high-quality luminescent QDs are usually synthesized in organic solvent, and the resulting QDs were capped with the native hydrophobic ligands such as trioctylphosphine oxide, therefore, they are insoluble in aqueous solutions (Qu and Peng 2002; Smith et al. 2008a; Xie et al. 2005). A number of QDs surface coating methods have been used, which include silica coating (Bruchez et al. 1998; Hu and Gao 2010; Schroedter et al. 2002), encapsulation with amphiphilic polymers (most commercial water-soluble QDs) (Kim et al. 2005; Pellegrino et al. 2004; Uskoković and Drofenik 2005), and ligand replacement with hydrophilic ligands (Chan and Nie 1998; Liu et al. 2007; Smith and Nie 2008). Silica shell coating and amphiphilic polymer encapsulation provide QDs with good aqueous solubility and preserve high photoluminescence quantum yields. However, this approach is complex and usually results in large hydrodynamic diameters of 30–50 nm (Chan and Nie 1998; Hu and Gao 2010; Liu et al. 2007; Smith and Nie 2008), which are often much larger than the cellular receptors being labeled, and become a barrier for the widespread application of QDs in biomedical imaging. Due to the particularly strong affinity of sulfur for the metallic cations on the surface of QDs, mercaptopropionic acid (MPA) (Chan and Nie 1998) and cysteine (Liu et al. 2007) are widely used as phase transfer reagents for QDs, owing to its simplicity, speed, and smaller size. Nevertheless, the colloidal stability is still limited due to the poor protection and drastic decrease in the quantum yields of the resulting water-soluble QDs. Thus, how to obtain water-soluble QDs with high quantum yield and high stability remains a great challenge.

Another way to make QDs water soluble is through multidentate polymer coating by ligand exchange, which usually produces compact QDs with high colloidal stability, with different combinations of polymer backbone, anchoring groups and pendant groups (Duan et al. 2010; Giovanelli et al. 2012; Liu et al. 2009, 2010; Palui et al. 2011; Smith and Nie 2008; Stewart et al. 2010; Wu et al. 2010; Yildiz et al. 2009, 2010; Zhang et al. 2012). However, further bioconjugation is needed since there are not any recognition sites on common polymers, which will increase the size of QDs and make the experiment too complicated. Therefore, if one can realize both specific targeting and good stability as well as biocompatibility through one surface modification step, it would be very convenient for the further biomedical application of QDs.

Hyaluronic acid (HA), which is a natural polysaccharide abundant in extracellular matrix, has been widely used in skin care (Gold 2007; Kerscher et al. 2008) and wound healing (Jang et al. 2014; Wang et al. 2006) due to its intrinsic physicochemical and biological properties including great water retention ability and biocompatibility. HA is also reported to selectively bind with CD44 receptor which is overexpressed in many cancers of epithelial origin (Platt and Szoka 2008) such as ovarian carcinoma (Luo and Prestwich 1999) and breast adenocarcinoma (Coradini et al. 1999). Owing to these unique features, HA has been used for development of the targetable carriers to deliver the therapeutic agents such as drug delivery (Yadav et al. 2008) and siRNA delivery (Hosseinkhani et al. 2013; Jiang et al. 2009; Lee et al. 2007) as well as imaging agents (Chen et al. 2014; Saravanakumar et al. 2014). Additionally, HA also contains derivable functional groups along its backbone. For instance, the carboxyl groups are good sites to be conjugated with thiol-containing cysteamine for QD surface binding. Based on all these considerations, here we established a facile one-step reverse micelle method to obtain HA-cysteamine polymer-coated QDs. The water solubility and stability in wide pH range were tested. Furthermore, its cytotoxicity as well as cancer cell-targeting ability was also investigated.

Materials and methods

Chemicals and instruments

Sodium hyaluronate with MW of 7500 was purchased from Lifecore (USA). Cystamine dihydrochloride, dithiothreitol (DTT), cyclohexane, IGEPAL CO-520, tetramethylammonium hydroxide (TMAH), ethylenediaminetetraacetic acid (EDTA), and Ellman's reagent were purchased from Sigma-Aldrich. EDC, sulfo-NHS, and cysteine hydrochloride monohydrate were purchased from Pierce. UV–Vis absorption spectra

were obtained using a Cary 100 Bio UV–Visible Spectrophotometer from Varian Company. Photoluminescence spectra were recorded by a Fluoromax 2 spectrofluorometer. Dynamic light scattering measurements were performed on a Brookhaven 90Plus Particle size analyzer. Transmission electron microscopy was performed on a Hitachi H-7500 TEM at the Electron Microscopy Core Facility at Emory University. 96-well plates were read by a Synergy 2 Multi-Mode Microplate Reader (Biotek, USA).

Synthesis of HA-cysteamine polymer

The synthesis of HA-cysteamine polymer involves two steps: synthesis of HA-cystamine polymer and reduction of the disulfide bond of cystamine by DTT. Typically, sodium hyaluronate with average MW of 7500 was dissolved in PBS, then 18 molar excess of EDC and 18 molar excess of sulfo-NHS were added to the HA sodium salt solution, and the mixture was stirred for 1 h to activate the carboxyl groups. Then 12 molar excess of cystamine dihydrochloride in PBS was added dropwise while stirring, and the mixture was kept reacting overnight. The HA-cystamine product was purified by dialyzing against 1X PBS buffer using MWCO 3500 dialysis tube. For DTT reduction of the disulfide bond on cystamine, 5 molar excess of DTT was added to HA-cystamine solution and stirred for 24 h. The final product was purified by dialyzing against pH 3 buffer using MWCO 3500 dialysis tube. The water was removed by lyophilizing for 2–3 days. Finally cotton-like HA-cysteamine polymers were obtained. The final product should be stored at −20 °C to protect the active thiol groups from being oxidized.

Determination of reactive thiols on HA-cysteamine polymer

The sulfhydryl group concentration on HA-cysteamine polymer was determined via Ellman's reagent by comparing to a standard curve composed of known concentrations of cysteine. Namely, 0.1 M sodium phosphate buffer of pH 8 containing 1 mM EDTA was prepared as reaction buffer. 4 mg Ellman's Reagent was dissolved in 1 ml of reaction buffer as Ellman's reagent solution. A set of cysteine standards were prepared by dissolving cysteine hydrochloride monohydrate at concentrations of 0, 0.25, 0.5, 0.75, 1, 1.25, and 1.5 mM in reaction buffer. 250 µl of each cysteine standard or HA-cysteamine polymer of known weight was added to separate test tubes which contain 50 µl of Ellman's reagent solution and 2.5 ml of reaction buffer. The mixture was incubated at room temperature for 15 min. Then the absorbance at 412 nm was measured using a plate reader and the standard curve was plotted. Finally, the active thiol group concentration of the HA-cysteamine polymer was determined accordingly.

Synthesis of (CdSe)CdZnS QDs and encapsulation with HA-cysteamine polymer

(CdSe)CdZnS QDs of 645 nm emission wavelength were synthesized following previous methods (Qu and Peng 2002; Xie et al. 2005). When encapsulating QDs with HA-cysteamine polymer, a modified reverse micelle method was used (Jana et al. 2010; Ying and Zarur 2002). Typically, 0.64 nmol QDs in hexane were dried by vacuum to get a thin film, then 9 ml cyclohexane was added until the QDs were fully dissolved. Next 1 ml IGEPAL CO-520, 10 mg HA-cysteamine polymer in 500 µl water and 3.61 mg TMAH in 200 µl methanol were added to form reverse micelle. The solution should be clear after adding all these reagents. If not clear, add more IGEPAL CO-520 or water. The mixture was sonicated for 5 min, and votexed for 60 min. Then 1–2 ml ethanol was added to precipitate the HA polymer-coated QDs. The pellets were washed with additional ethanol for 3 times and re-dispersed in 1X PBS. After centrifuging the QDs solution at $5{,}000\times g$ for 10 min to get rid of the undissolved parts, the supernatant which contains the HA polymer-coated QDs was purified using a 0.2 µm syringe filter.

pH stability test

A "universal" pH buffer, Britton–Robinson buffer, with pH range of 2–12 was prepared (Britton and Robinson 1931). Then a same amount of concentrated HA polymer-coated QDs were added to each pH solution. The QDs solution was added in fluorescence testing tubes and sealed well with parafilm. After 1 h, 16 h, and 24 h incubation at room temperature, the photoluminescence of QDs was recorded by a fluorometer, and integrated intensity was calculated for comparison. The fluorescence intensity of QDs in pH 7

buffer after 1 h incubation was referenced as 1, and others were scaled as certain percent ratio. The corresponding fluorescence images of QDs after 24 h incubation were taken by illuminating with a 365 nm hand-held UV lamp.

Long-time stability test

Long-time stability of the HA polymer-coated QDs was tracked for 5 months and compared with mercaptoacetic acid (MAA)-coated QDs. Typically, 300 μl HA polymer-coated QDs in 1X PBS buffer at a concentration of 25 nM was added in a fluorescence testing tube and sealed well with parafilm. The QDs-containing tube was stored in 4 °C refrigerator and the fluorescence intensity was tested on certain days. To prepare MAA-coated QDs, 150 μl QDs of 10 nM in crude stock was precipitated with 13 ml acetone. The pellets were washed with acetone and re-dispersed in 1 ml chloroform. 500 μl MAA and 100 mg TMAH in 500 μl methanol were added. The whole solution was sonicated for 10 min and kept at 60 °C water bath for 1 h. The QDs were precipitated with acetone by centrifuge at 8,000×g for 10 min, washed with acetone, and dissolved in 1X Borate buffer. The QDs were dialyzed against 50 mM borate buffer (pH 8.5) using 20 K MWCO dialysis tube, and then stored at 4 °C in the dark. The fluorescence intensity was integrated for each spectrum and compared with the first day's result.

Cell culture medium stability test

The stability of HA polymer-coated QDs in cell culture medium was tested and compared with the commercial carboxyl 655 nm QDs from Invitrogen. Typically, the HA polymer-coated QDs and 655 nm carboxyl QDs from Invitrogen were diluted in PBS or DMEM phenol red-free medium with 10 % fetal bovine serum (FBS) added. The QDs were sealed and put under room temperature without any protection from light. At 0, 1, 16, and 24 h, the fluorescence of these QDs was tested and integrated. The integrated fluorescence intensity of each QDs in PBS at 0 h was set as 1 and all results were referenced to get certain percent ratio.

Cytotoxicity test

MD-MB-231 breast cancer cell line was cultured in RPMI 1640 with 10 % FBS and 1 % streptomycin and penicillin antibiotics. On the first day, cells were seeded on a 96-well plate at 5×10^3 cells/well. After 24 h culture, HA polymer-coated QDs were added to the 4, 10, and 25 h incubation time group with the final concentrations of 1, 5, 10, and 20 nM. For the control group, cells of same number were seeded but no QDs were added. This is regarded as 100 % cell viability. A blank control with only cell culture medium in the well was regarded as 0 % cell viability. Experiments were triplicated. After incubation with QDs, the medium was aspirated and 100 μl of new cell culture medium and 10 μl Cell Counting Kit-8 solution was added to each well. Following incubation with cells at 37 °C for 3 h, the absorbance at 450 nm was measured by a plate reader.

Cancer cell-targeted imaging

$CD44^+$ MD-MB-231 and MCF-7 breast cancer cells were used for targeted imaging and NIH/3T3 fibroblast cell was used as a negative control. Due to the different growth speed, NIH/3T3 fibroblast cells were seeded at 3500 cell/well and MD-MB-231 and MCF-7 breast cancer cells were seeded at 25×10^3 cell/well on 8-well chamber slides. After 24 h growth, cells were washed with 1X PBS buffer and then fixed with 200 μl 4 % formaldehyde and 0.25 % Triton X-100 in PBS for each well. After 15 min, cells were washed with PBS for 5 min, three times. 200 μl blocking buffer of 6 % bovine serum albumin (BSA) in PBS was added to each well and incubated for 1 h. Then blocking buffer was aspirated and 200 μl HA polymer-coated QDs were added to each well, with final concentrations of 1, 5, 10, and 20 nM in blocking buffer. After 1 h incubation, each well was washed with PBS three times for 5 min each. The slides were mounted with anti-fade mounting media containing DAPI. The slides were imaged under Olympus IX71, using 20X objective.

Hyaluronic acid competitive inhibition test

MCF-7 cells were seeded on an 8-well chamber slide at 30 k/well for overnight growth. The fixation, permeabilization, and blocking procedure are the same with the targeted imaging experiment. Before adding QDs, different concentrations of 200 μl HA in blocking buffer were added to each well for 1 h. HA concentrations used are 0 nM (as control), 10 nM,

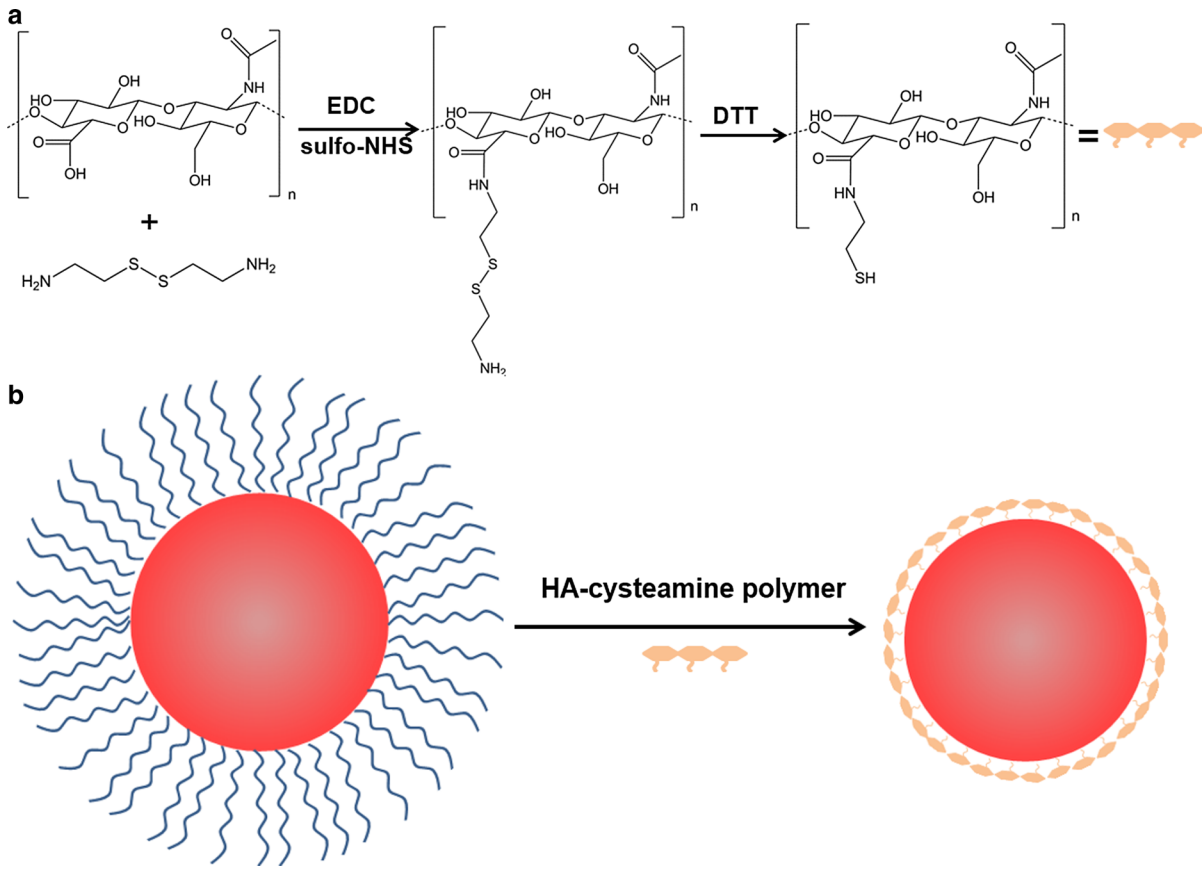

Fig. 1 Preparation of HA-cysteamine polymer-coated QDs. **a** The chemical synthesis of HA-cysteamine polymer. **b** Schematic illustration of HA polymer coating on QDs

100 nM, 1 μM, 10 μM, 100 μM, 1 mM, and 10 mM. Then HA solution was aspirated and 200 μl HA polymer-coated QDs at final concentration of 10 nM in blocking buffer were added to each well. After 1 h incubation, the QDs were washed with PBS and mounted, and the slide was imaged under Olympus IX71, using a 20X objective.

Results

Synthesis and characterization of HA-cysteamine polymer

As shown in Fig. 1a, the amine group of cystamine was first covalently conjugated to the carboxyl group on HA using EDC and sulfo-NHS. Then the disulfide bond of cystamine was further reduced with DTT to get the final HA-cysteamine polymer. Each polymer molecule contains approximately 8 active thiols, as determined via Ellman's method. Averagely, an HA molecule with MW 7500 contains about 19 carboxyl groups, therefore, about 42 % carboxyl groups on HA have been converted to thiol groups. This thiol modification ratio can ensure strong binding of the HA polymer on QDs surface and also a large amount of carboxyl groups are left to maintain the HA targeting ability for CD44 receptor on cell surface.

Preparation and characterization of HA-cysteamine polymer-coated QDs

HA Polymer-coated QDs were synthesized using an adapted reverse micelle method for ligand exchange and phase transfer reaction (Jana et al. 2010; Ying and Zarur 2002) as shown in Fig. 1b. Hydrophobic QDs protected with oleylamine on surface were synthesized by traditional methods (Qu and Peng 2002; Xie et al. 2005). For

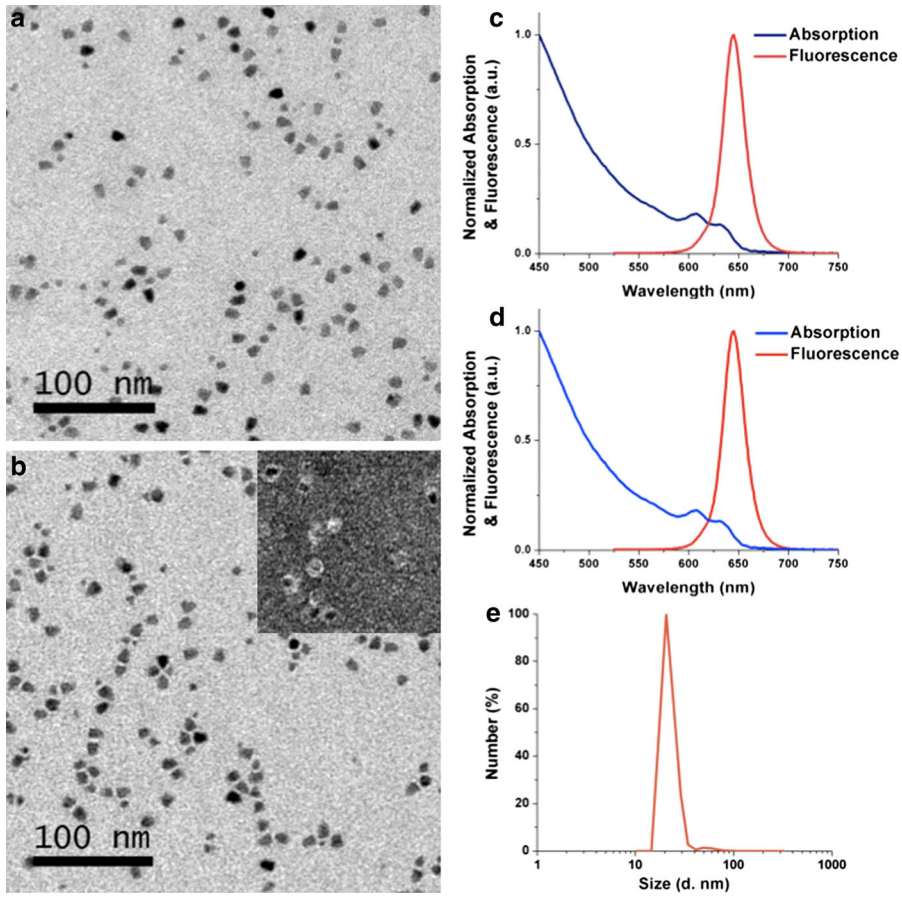

Fig. 2 Characterization of QDs. **a** TEM image of QDs in hexane (before polymer coating). **b** TEM images of HA-cysteamine polymer-coated QDs in water. Negative staining TEM is inserted with the same *scale bar*, showing the polymer coating layer. **c** Absorption and fluorescence spectra of QDs in hexane (before polymer coating). **d** Absorption and fluorescence spectra of QDs after HA-cysteamine polymer coating, showing no significant difference with the spectra before polymer coating. **e** DLS size distribution showing a peak hydrodynamic diameter of ~22.6 nm

ligand exchange, the hydrophobic QDs were first dispersed in cyclohexane. With the addition of IGEPAL CO-520 and HA-cysteamine polymer dissolved in water, a reverse micelle was formed. TMAH was used as a phase transfer catalyst to induce the reaction. After the reaction, water-soluble QDs coated with HA-cysteamine polymer were incorporated inside the reverse micelle. Figure 2a, b shows representative transmission electron microscopy (TEM) images of QDs before and after polymer coating. Both of them appear uniform in size and were well dispersed. Figure 2a shows the crystal size of QDs before polymer coating is 9.5 ± 1.3 nm. Negative staining TEM with 1 % methylamine tungstate clearly shows polymer-coated QDs with a thin layer as shown in the inserted plot of Fig. 2b and the overall size of HA-coated QDs is 14.5 ± 1.6 nm. Figure 2c, d shows UV absorption and fluorescence spectra before (Fig. 2c) and after (Fig. 2d) the HA polymer coating. We can see that there is no significant difference among the 2 sets of spectra. Quantum yield (QY) calculation was 24 % after coating, while the QY of QDs in hexane before coating is 28.1 %. The QY did not lose much after polymer coating, which proves a good surface protection and passivation. The dynamic light scattering (DLS) results (Fig. 2e) show that the hydrodynamic size of the compact HA polymer-coated QDs is around 22.6 ± 5.2 nm.

To exclude the possibility that the hydrophobic part of IGEPAL CO-520 intercalates into oleylamine on QD surface, and the hydroxyl groups render QDs water soluble, control experiment without adding HA-cysteamine polymer was conducted. The final QDs pellets cannot dissolve in water, which proved that it is HA polymer rather than IGEPAL CO-520 that makes QDs water soluble.

pH stability test

The colloidal stability of HA polymer-coated QDs in different pH buffer from 2 to 12 was tested. As shown in Fig. 3a, the polymer-coated QDs keep great

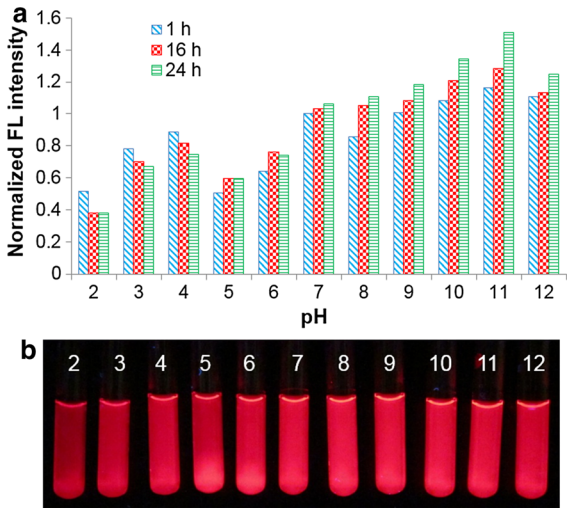

Fig. 3 pH stability of HA-cysteamine polymer-coated QDs. **a** Normalized integrated fluorescence intensity after incubating for 1, 16, and 24 h in different pH buffer. The fluorescence intensity of QDs in pH 7 buffer after 1 h incubation was referenced as 1. **b** Corresponding fluorescence images of QDs after 24 h incubation (illuminated with a 365 nm hand-held UV lamp)

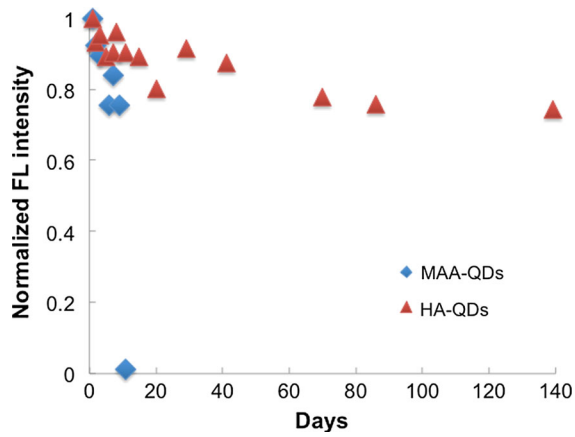

Fig. 4 Long-time stability of HA-cysteamine polymer-coated QDs, compared with MAA-coated QDs. The MAA-coated QDs precipitated after 11 days thus lose its fluorescence totally

fluorescence performance even after as long as 24 h incubation with the extreme pH condition. The QDs have better fluorescence performance in basic buffer than in acidic buffer. As the incubation time increases at each pH, integrated fluorescence in acidic buffer gradually decreases while in basic buffer it increases. This is reasonable considering that the HA has unmodified carboxyl groups, which makes them more soluble in basic solution. However, we can see from Fig. 3b that after 24 h incubation the QDs did not precipitate or aggregate and still keep great colloidal and photo stability even for as long as 24 h incubation with pH range from 2 to 12. This indicates that the HA polymer-coated QDs can adapt to the complex body environment of different pH changes, and they can be good candidates as intracellular and in vivo imaging probes for lone-time tracking.

Long-time stability test

Long-time stability of the HA polymer-coated QDs was tracked for 5 months. For the same vial of 25 nM QDs in 1X PBS buffer stored at 4 °C, the integrated fluorescence intensity did not drop much even after as long as 140 days, while a control group using MAA-coated QDs stored at the same condition precipitated within 11 days, as shown in Fig. 4. The HA polymer-coated QDs show great long-time stability comparing with the single-thiol MAA-coated QDs. This is a good example showing the necessity of using multi-thiol polymer coating.

Stability in cell culture medium

The QDs stability in FBS containing cell culture medium is very important for further cellular and even in vivo imaging applications. If the fluorescence of QDs is easily affected, then it will be hard to obtain stable and quantitative continues imaging. The results of the HA polymer-coated QDs were shown in Fig. 5a. We can see that those QDs keep excellent fluorescence stability in cell culture medium at room temperature without any protection from the light, and the stability of our HA polymer-coated QDs is comparable to the commercial carboxyl QDs from Invitrogen (Fig. 5b). The results proved the great cell culture medium stability of the HA polymer-coated QDs and showed the possibility for further cellular applications.

Cytotoxicity test

The cytotoxicity of HA polymer-coated QDs was examined in MD-MB-231 breast cancer cells. QDs of different final concentrations of 1, 5, 10, and 20 nM were incubated with the cells for 4, 10, and 25 h. This is in the typical concentration range for cellular

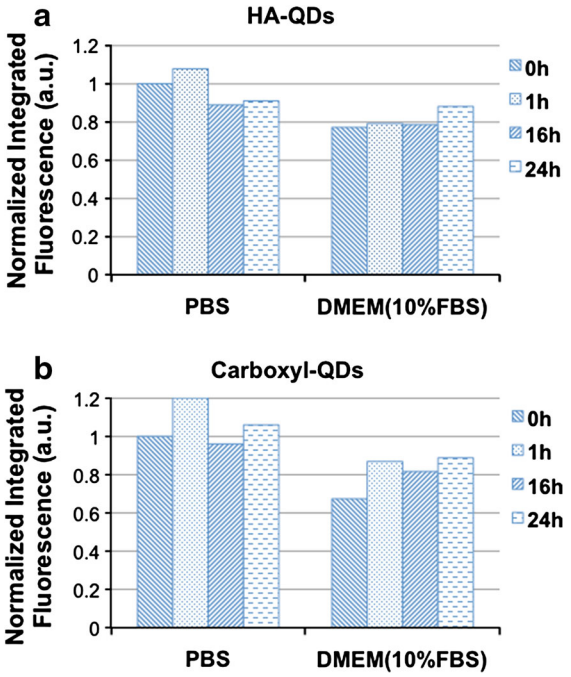

Fig. 5 Stability in cell culture medium of HA polymer-coated QDs and commercial carboxyl QDs from Invitrogen

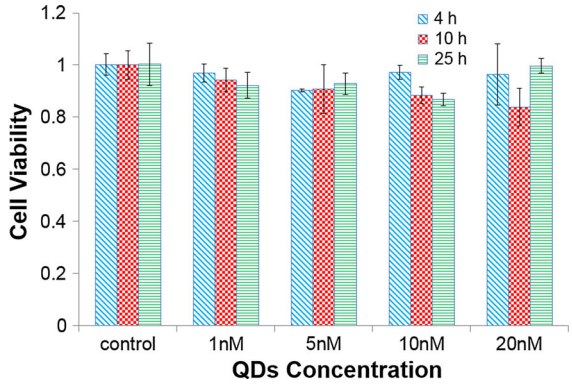

Fig. 6 Cytotoxicity test of HA-cysteamine polymer-coated QDs. Dose-dependent viability evaluation of MD-MB-231 breast cancer cells treated for 4, 10, and 25 h. The experiments were performed in triplicate

staining with QD bioconjugates (Medintz et al. 2005) and the tested incubation time is long enough for QDs in vivo imaging conditions (Smith et al. 2008a). The experiments were performed in triplicate and *T* test was performed for each group comparing to the control group. As shown in Fig. 6, no significant cytotoxicity was observed at all concentration and incubation time groups. Even after 24 h incubation at 20 nM concentration, the cell viability remains over 83 %. This result has proved great biocompatibility for the HA polymer-coated QDs, and shows the potential for in vivo applications in the future.

$CD44^+$ cancer cell-targeted imaging

$CD44^+$ MCF-7 and MD-MB-231 cell lines were used for targeted imaging and NIH/3T3 cell line was used as a negative control. HA polymer-coated QDs with different final concentrations of 5 and 10 nM have been tested, and shown in Fig. 7. Obviously, strong fluorescence on MD-MB-231 and MCF-7 cell lines was observed but no fluorescence on NIH/3T3 cell line can be seen. This result not only demonstrates the targeted ability of the polymer-coated QDs, but also indicates very little non-specific cellular binding for NIH/3T3 cell. Therefore, for future studies, final concentration of 5 nM QDs will be high enough for HA-targeted imaging.

Hyaluronic acid receptor competitive imaging

In order to confirm that the staining of breast cancer cell line is receptor mediated, we conducted an HA competitive imaging experiment on MCF-7 cell by treating the cells with different concentrations of HA before adding of HA polymer-coated QDs. As presented in Fig. 8, when HA concentration increases, the QDs fluorescence intensity shows a downward trend and QD fluorescence could not be detected at 10 μM HA treating dosage. This result is a solid evidence to prove that the mechanism of HA polymer-coated QDs to stain the cells is mediated by the HA receptor.

Discussion

The current established one-step QDs modification method is advantageous in the following three aspects. Firstly, for biomedical applications, a targeting moiety like antibody, peptide, or small molecule should be added to the surface modified QDs, so that QDs can be used to target tumor biomarkers as well as tumor vasculatures with high affinity and specificity (Smith et al. 2008a). Because most of the surface coating itself

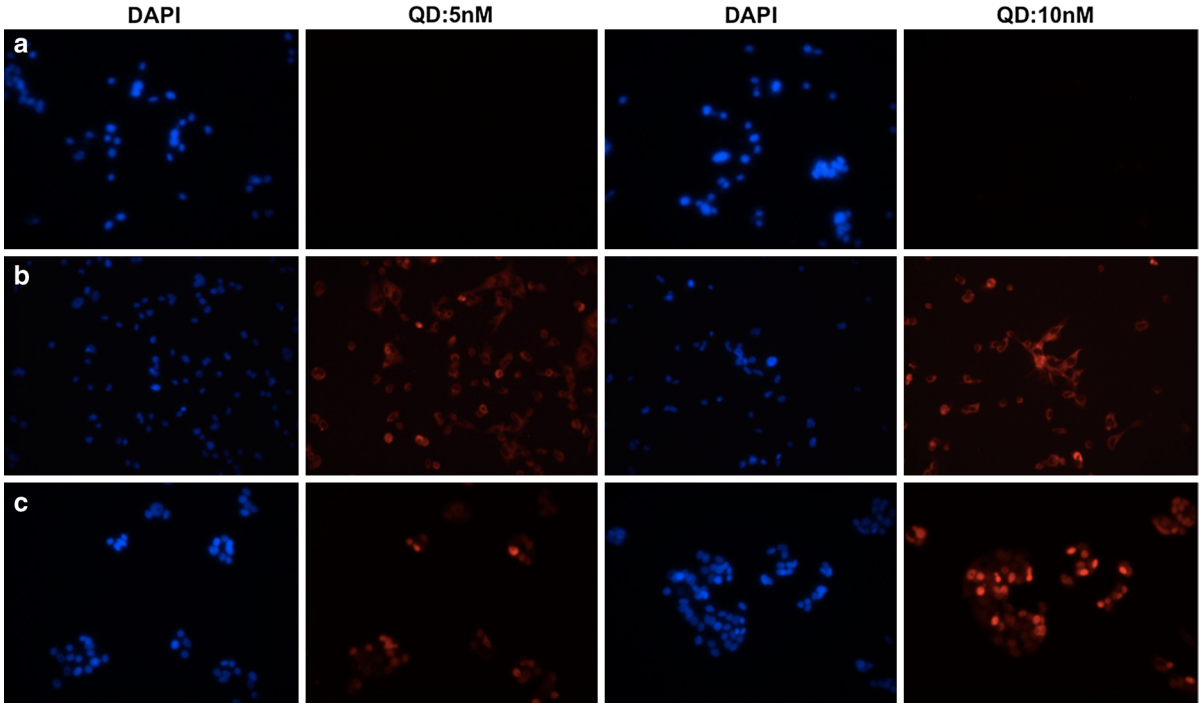

Fig. 7 Illustration of the targeted imaging of breast cancer cells with HA-cysteamine polymer-coated QDs with final concentration of 5 and 10 nM. **a** NIH/3T3 fibroblast cell line shows no QD fluorescence and little non-specific cellular binding. **b** MDMB-231 breast cancer cell line shows strong QD fluorescence of targeted staining. **c** MCF-7 breast cancer cell line also shows strong QD fluorescence of targeted staining. 20X objective was used on an Olympus IX 71 microscope

does not have targeting ability, a following bioconjugation step is necessary. However, it is always time consuming and usually increases the overall size of QDs. Comparing with previous multidentate polymer coating methods (Duan et al. 2010; Giovanelli et al. 2012; Liu et al. 2009, 2010; Palui et al. 2011; Smith and Nie 2008; Stewart et al. 2010; Wu et al. 2010; Yildiz et al. 2009, 2010; Zhang et al. 2012), the current method is much simplified. By employing the HA polymer as the coating molecules, we have circumvented the targeting moiety conjugation step, and produced QDs with not only small size, but also CD44 receptor recognition groups, namely the carboxyl groups on HA.

Secondly, the traditional QDs coating methods, such as single-thiol (Chan and Nie 1998; Liu et al. 2007) and di-thiol coating (Clapp et al. 2006), could not protect the QDs surface very well thus the resulting stability is not good enough. And their applications for in vivo imaging are hampered by their sensitivity to biochemical environments. In order to get more stable QDs, recent efforts have been directed toward synthesizing ligands or polymers with multiple functional groups with different backbones and pendant groups. For instance, poly (methacrylate) (Giovanelli et al. 2012; Liu et al. 2009; Yildiz et al. 2009, 2010), poly (acryl acid) (PAA) (Liu et al. 2010; Palui et al. 2011; Smith and Nie 2008), and poly (maleic anhydride) (Duan et al. 2010; Zhang et al. 2012) are the most frequently used backbones. DHLA (Giovanelli et al. 2012; Palui et al. 2011; Stewart et al. 2010; Wu et al. 2010; Yildiz et al. 2009, 2010) and cysteamine (Duan et al. 2010; Liu et al. 2010; Smith and Nie 2008) are mostly used as anchoring group, and polyethylene glycol (PEG) (Duan et al. 2010; Liu et al. 2009; Palui et al. 2011; Stewart et al. 2010; Yildiz et al. 2009, 2010; Zhang et al. 2012) is often used as pendant group to increase water solubility and minimize nonspecific cellular binding. However, the reported pH stability is still in a limited range and short time. For instance, polyPEG QDs were incubated at room temperature for 4 h in a pH range of 5–10.5 (Liu et al. 2009), or for days over a pH range of 5.0–9.0 (Yildiz et al. 2009). In this work, a wide pH range of

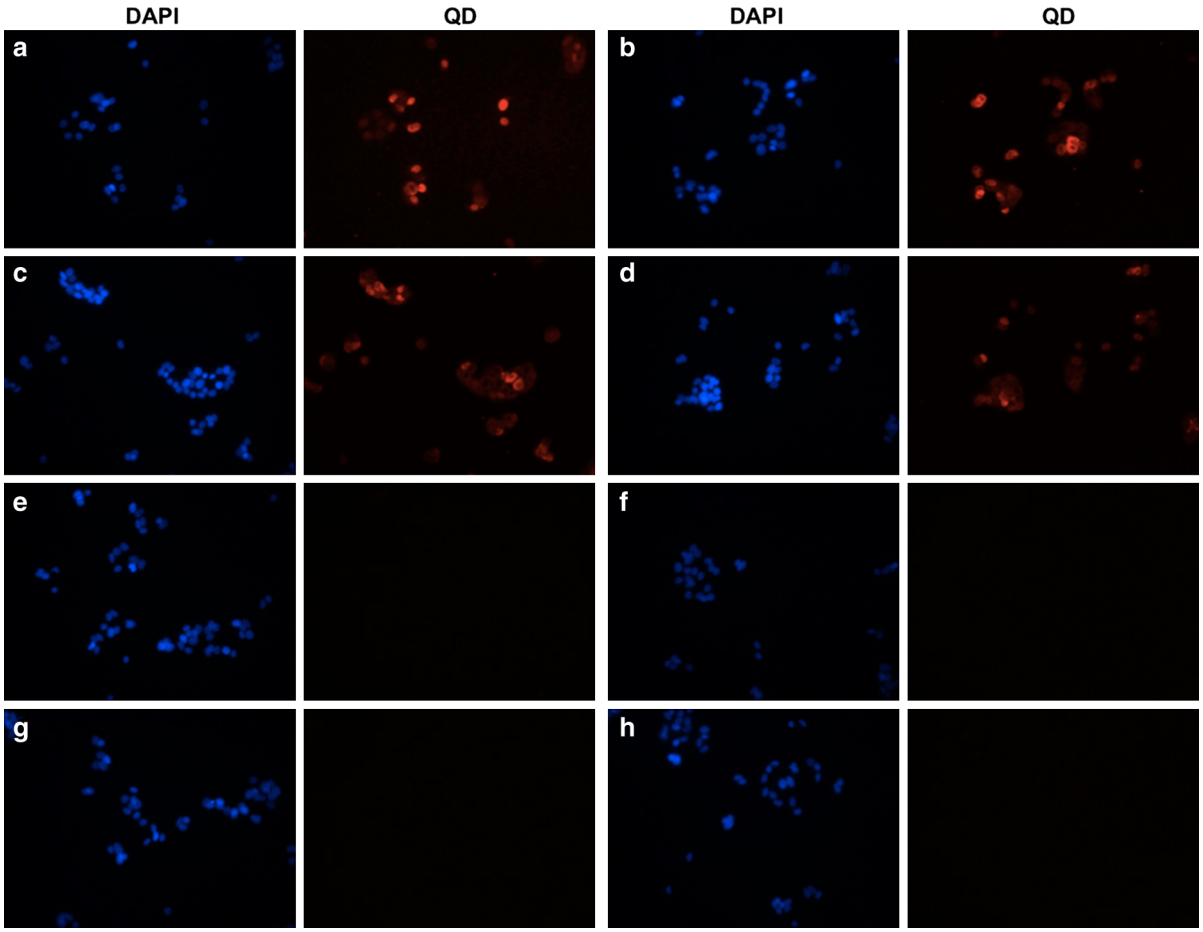

Fig. 8 HA receptor competitive targeted imaging of MCF-7 cell line with HA-cysteamine polymer-coated QDs treated with different concentrations of HA. **a** Control group (no HA), **b** 10 nM, **c** 100 nM, **d** 1 μM, **e** 10 μM, **f** 100 μM, **g** 1 mM, **h** 10 mM. QD final concentration was 10 nM for all. 20X objective was used on Olympus IX 71 microscope. From 1 to 10 μM HA, QD fluorescence intensity has a dramatic change, which indicates that the staining is mediated by HA receptor

2–12 has been tested with as long as 24 h incubation time, showing a great pH stability and potential to adapt to a more complex body environment. Besides, it is reported that SiO_2 and PE-PEG-coated QDs have remarkable stability among pH 1–14 (Hu and Gao 2010), however, the pH stability was recorded for only 1 h. And the size of the modified QDs is as large as 40–50 nm. These QDs are good candidates for pH sensing, but may not be very suitable for biological application since further bioconjugation will undoubtedly increase the overall size.

Thirdly, the introduction of reverse micelle can prevent QDs aggregation and help keeping good dispersity. This has been demonstrated by the TEM images and the DLS analysis. The reason is that the reverse micelles are tiny droplets of water encapsulated by the surfactant molecules IGEPAL CO-520 and thus physically separated from the cyclohexane oil phase. This water-in-oil microemulsion provides microreactors for QDs coating with hydrophilic cysteamine-HA molecules, therefore, allows excellent control of the particle size, shapes, homogeneity, and negligible contamination of the product compared with other bulk wet approaches like traditional biphasic exchange method with thiol-containing molecule and polymers (Liu et al. 2007; Smith and Nie 2008).

It is notable that HA targets the cell receptor through the carboxyl groups, therefore, the modification ratio of carboxyl groups on HA is very important.

People have done a series of work using adipic acid dihydrazide-modified HA to conjugate commercial carboxyl Quantum Dots for in vivo imaging, and found that lower carboxyl-modified HA (i.e., 35, 22 %) kept the targeted ability for HA receptors in liver, while higher modification ratio (i.e. 50, 68 %) of HA will lose much of HA targeting ability (Kim et al. 2008, 2012). In our work, about 42 % of the carboxyl group on HA was modified and the $CD44^+$ cancer cell-targeted imaging test has proved that this ratio still works well for HA to keep the targeting ability for receptors.

Moreover, it has been proved in many studies that cytotoxicity of the surface modified QDs in vitro was dependent on the surface properties (Derfus et al. 2004; Gao et al. 2004; Hu and Gao 2010; Wu et al. 2002). Mercaptoundecanoic acid (MUA) CdSe QDs caused cell death after 4–6 h incubation at 0.2 mg/ml (Shiohara et al. 2004), as QDs stabilized by small ligands are highly prone to degradation due to the weakly protection (Cho et al. 2007; Lovrić et al. 2005). Less toxic QDs are obtained by encapsulated in amphiphilic polymers or cross-linked silica. Previous work using silica to coat QDs showed mild cytotoxicity and the cell viability was 86 % (C6 cells) and 77.7 % (HepG2 cells) at 100 μg/ml, but only 4 h incubation time was tested (Durgadas et al. 2012). Another work was a combination of silica and amphiphilic PEG polymer-coated QDs. The cell viability is above 80 % after incubation for 24 h when the QDs concentration is less than 100 μg/ml (approximately 6 nM). However, at elevated concentrations (e.g., 500 μg/ml, ~30 nM), cell viability decreases to less than 60 % after 24 h incubation (Hu and Gao 2010). As a biocompatible polysaccharide, HA has been applied to reduce the cytotoxicity of nanoparticles. For instance, HA has been used to immobilize magnetic nanoparticles and the result shows that the cell viability was higher than 80 % at 50 μg/ml for as long as 24 h (Kamat et al. 2010). Also, QD-labeled collagen/HA porous scaffolds have been fabricated and 10 nM of QDs exhibited no cytotoxic effect on fibroblasts for as long as 72 h (Cheng et al. 2012). These studies coincide with our cytotoxicity results of HA polymer-coated QDs and proved the biocompatibility of HA coating similarly. Of course, long-term and systematic in vivo toxicity investigation are still essential before further in vivo applications.

Conclusions

In conclusion, we have successfully developed a novel HA-cysteamine polymer to coat QDs which provides strong binding of the polymer to the nanocrystal's surface via its multiple-thiol groups. The resulting QDs have great water solubility, and excellent colloidal stability for long time and over a large pH range from 2 to 12. The HA polymer-coated QDs also show great biocompatibility and no significant toxicity and high stability in biological environments. Moreover, the HA polymer-coated QDs hold $CD44^+$ cancer cell-targeting ability for breast cancer cell lines. Although only breast cancer cell lines were tested in this work, we can expect the potential application of HA polymer-coated QDs for other CD44 receptor over-expressed cancer cell lines such as ovarian carcinoma, colon carcinoma, and murine melanoma. Besides, the carboxyl groups on the polymer backbone also allow for further functionalization and conjugation with other targeting probes like ligands or antibodies. Therefore, the HA-polymer coated QDs can be applied for variety of biomarkers detection such as multiplexed biomarker staining, live cell imaging, long-time single QDs tracking, and moreover, for in vivo molecular imaging as well as targeted drug delivery.

Acknowledgments We acknowledge the financial support by the Wallace H. Coulter GT/Emory-PKU BME collaborative research seed grant program and the National Key Instrumentation Development Project (2011YQ030114), as well as Guangdong Innovative Research Team Program (No. 2011S090). We also thank Dr. Andrew M. Smith for kindly providing the QDs.

References

Britton HTS, Robinson RA (1931) CXCVIII.—Universal buffer solutions and the dissociation constant of veronal. J Chem Soc 1:1456–1462

Bruchez M, Moronne M, Gin P, Weiss S, Alivisatos AP (1998) Semiconductor nanocrystals as fluorescent biological labels. Science 281:2013–2016

Chan WCW, Nie S (1998) Quantum dot bioconjugates for ultrasensitive nonisotopic detection. Science 281:2016–2018

Chan WCW, Maxwell DJ, Gao X, Bailey RE, Han M, Nie S (2002) Luminescent quantum dots for multiplexed biological detection and imaging. Curr Opin Biotech 13:40–46

Chen B, Miller RJ, Dhal PK (2014) Hyaluronic acid-based drug conjugates: state-of-the-art and perspectives. J Biomed Nanotechnol 10:4–16

Cheng H-T, Chuang E-Y, Ma H, Tsai C-H, Perng C-K (2012) Fabrication of quantum dot-conjugated collagen/hyaluronic acid porous scaffold. Ann Plast Surg 69:663–667

Cheng Y, Zhao Y, Shangguan F, Ye B, Li T, Gu Z (2014) Convenient generation of quantum dot-incorporated photonic crystal beads for multiplex bioassays. J Biomed Nanotechnol 10:760–766

Cho SJ, Maysinger D, Jain M, Röder B, Hackbarth S, Winnik FM (2007) Long-term exposure to CdTe quantum dots causes functional impairments in live cells. Langmuir 23:1974–1980

Clapp AR, Goldman ER, Mattoussi H (2006) Capping of CdSe–ZnS quantum dots with DHLA and subsequent conjugation with proteins. Nat Protoc 1:1258–1266

Coradini D, Pellizzaro C, Miglierini G, Daidone MG, Perbellini A (1999) Hyaluronic acid as drug delivery for sodium butyrate: improvement of the anti-proliferative activity on a breast-cancer cell line. Int J Cancer 81:411–416

Derfus AM, Chan WC, Bhatia SN (2004) Probing the cytotoxicity of semiconductor quantum dots. Nano Lett 4:11–18

Duan HW, Kuang M, Wangi YA (2010) Quantum dots with multivalent and compact polymer coatings for efficient fluorescence resonance energy transfer and self-assembled biotagging. Chem Mat 22:4372–4378

Durgadas CV, Sreenivasan K, Sharma CP (2012) Bright blue emitting CuSe/ZnS/silica core/shell/shell quantum dots and their biocompatibility. Biomaterials 33:6420–6429

Gao X, Cui Y, Levenson RM, Chung LWK, Nie S (2004) *In vivo* cancer targeting and imaging with semiconductor quantum dots. Nat Biotechnol 22:969–976

Giovanelli E, Muro E, Sitbon G, Hanafi M, Pons T, Dubertret B, Lequeux N (2012) Highly enhanced affinity of multidentate versus bidentate zwitterionic ligands for long-term quantum dot bioimaging. Langmuir 28:15177–15184

Gold MH (2007) Use of hyaluronic acid fillers for the treatment of the aging face. Clin Interv Aging 2:369

Hosseinkhani H, He W-J, Chiang C-H, Hong P-D, Yu D-S, Domb A, Ou K-L (2013) Biodegradable nanoparticles for gene therapy technology. J Nanopart Res 15:1–15

Hu X, Gao X (2010) Silica-polymer dual layer-encapsulated quantum dots with remarkable stability. ACS Nano 4:6080–6086

Jana NR, Erathodiyil N, Jiang J, Ying JY (2010) Cysteine-functionalized polyaspartic acid: a polymer for coating and bioconjugation of nanoparticles and quantum dots. Langmuir 26:6503–6507

Jang YL et al (2014) Hyaluronic acid-siRNA conjugate/reducible polyethylenimine complexes for targeted siRNA delivery. J Nanosci Nanotechnol 14:7388–7394

Jiang G, Park K, Kim J, Kim KS, Hahn SK (2009) Target specific intracellular delivery of siRNA/PEI-HA complex by receptor mediated endocytosis. Mol Pharm 6:727–737

Kamat M, El-Boubbou K, Zhu DC, Lansdell T, Lu X, Li W, Huang X (2010) Hyaluronic acid immobilized magnetic nanoparticles for active targeting and imaging of macrophages. Bioconjugate Chem 21:2128–2135

Kerscher M, Bayrhammer J, Reuther T (2008) Rejuvenating influence of a stabilized hyaluronic acid-based gel of nonanimal origin on facial skin aging. Dermatol Surg 34:720–726

Kim S-W, Kim S, Tracy JB, Jasanoff A, Bawendi MG (2005) Phosphine oxide polymer for water-soluble nanoparticles. J Am Chem Soc 127:4556–4557

Kim J et al (2008) In vivo real-time bioimaging of hyaluronic acid derivatives using quantum dots. Biopolymers 89:1144–1153

Kim KS, Kim S, Beack S, Yang JA, Yun SH, Hahn SK (2012) In vivo real time confocal microscopy for target specific delivery of hyaluronic acid-quantum dot conjugates. nanomedicine: nanotechnology. Biol Med 8:1070–1073

Lee H, Mok H, Lee S, Oh YK, Park TG (2007) Target-specific intracellular delivery of siRNA using degradable hyaluronic acid nanogels. J Control Release 119:245–252

Leutwyler WK, Bürgi SL, Burgl H (1996) Semiconductor clusters, nanocrystals, and quantum dots. Science 271:933

Liu W, Choi HS, Zimmer JP, Tanaka E, Frangioni JV, Bawendi M (2007) Compact cysteine-coated CdSe (ZnCdS) quantum dots for in vivo applications. J Am Chem Soc 129:14530–14531

Liu W et al (2009) Compact biocompatible quantum dots via RAFT-mediated synthesis of imidazole-based random copolymer ligand. J Am Chem Soc 132:472–483

Liu L, Guo X, Li Y, Zhong X (2010) Bifunctional multidentate ligand modified highly stable water-soluble quantum dots. Inorg Chem 49:3768–3775

Lovrić J, Cho SJ, Winnik FM, Maysinger D (2005) Unmodified cadmium telluride quantum dots induce reactive oxygen species formation leading to multiple organelle damage and cell death. Chem Biol 12:1227–1234

Luo Y, Prestwich GD (1999) Synthesis and selective cytotoxicity of a hyaluronic acid-antitumor bioconjugate. Bioconjugate Chem 10:755–763

Medintz IL, Uyeda HT, Goldman ER, Mattoussi H (2005) Quantum dot bioconjugates for imaging, labelling and sensing. Nat Mater 4:435–446

Palui G, Na HB, Mattoussi H (2011) Poly(ethylene glycol)-based multidentate oligomers for biocompatible semiconductor and gold nanocrystals. Langmuir 28:2761–2772

Pellegrino T et al (2004) Hydrophobic nanocrystals coated with an amphiphilic polymer shell: a general route to water soluble nanocrystals. Nano Lett 4:703–707

Platt VM, Szoka FC Jr (2008) Anticancer therapeutics: targeting macromolecules and nanocarriers to hyaluronan or CD44, a hyaluronan receptor. Mol Pharm 5:474–486

Qu L, Peng X (2002) Control of photoluminescence properties of CdSe nanocrystals in growth. J Am Chem Soc 124:2049–2055

Ruan G, Agrawal A, Marcus AI, Nie S (2007) Imaging and tracking of tat peptide-conjugated quantum dots in living cells: new insights into nanoparticle uptake, intracellular transport, and vesicle shedding. J Am Chem Soc 129:14759–14766

Saravanakumar G, Deepagan V, Jayakumar R, Park JH (2014) Hyaluronic acid-based conjugates for tumor-targeted drug delivery and imaging. J Biomed Nanotechnol 10:17–31

Schroedter A, Weller H, Eritja R, Ford WE, Wessels JM (2002) Biofunctionalization of silica-coated CdTe and gold nanocrystals. Nano Lett 2:1363–1367

Shiohara A, Hoshino A, Hanaki Ki, Suzuki K, Yamamoto K (2004) On the cyto-toxicity caused by quantum dots. Microbiol Immunol 48:669–675

Smith AM, Nie S (2008) Minimizing the hydrodynamic size of quantum dots with multifunctional multidentate polymer ligands. J Am Chem Soc 130:11278–11279

Smith AM, Nie S (2011) Bright and compact alloyed quantum dots with broadly tunable near-infrared absorption and fluorescence spectra through mercury cation exchange. J Am Chem Soc 133:24

Smith AM, Duan H, Mohs AM, Nie S (2008a) Bioconjugated quantum dots for in vivo molecular and cellular imaging. Adv Drug Deliver Rev 60:1226–1240

Smith AM, Mohs AM, Nie S (2008b) Tuning the optical and electronic properties of colloidal nanocrystals by lattice strain. Nat Nanotechnol 4:56–63

Steponkiene S, Valanciunaite J, Skripka A, Rotomskis R (2014) Cellular uptake and photosensitizing properties of quantum dot-chlorin e 6 complex: in vitro study. J Biomed Nanotechnol 10:679–686

Stewart MH et al (2010) Multidentate poly(ethylene glycol) ligands provide colloidal stability to semiconductor and metallic nanocrystals in extreme conditions. J Am Chem Soc 132:9804–9813

Uskoković V, Drofenik M (2005) Synthesis of materials within reverse micelles. Surf Rev Lett 12:239–277

Wang TW, Sun JS, Wu HC, Tsuang YH, Wang WH, Lin FH (2006) The effect of gelatin-chondroitin sulfate-hyaluronic acid skin substitute on wound healing in SCID mice. Biomaterials 27:5689–5697

Wu X et al (2002) Immunofluorescent labeling of cancer marker Her2 and other cellular targets with semiconductor quantum dots. Nat Biotechnol 21:41–46

Wu YZ et al (2010) pH-Responsive quantum dots via an albumin polymer surface coating. J Am Chem Soc 132:5012–5014

Xie R, Kolb U, Li J, Basché T, Mews A (2005) Synthesis and characterization of highly luminescent CdSe-Core CdS/Zn0. 5Cd0. 5S/ZnS multishell nanocrystals. J Am Chem Soc 127:7480–7488

Xing Y et al (2007) Bioconjugated quantum dots for multiplexed and quantitative immunohistochemistry. Nat Protoc 2:1152–1165

Yadav AK, Mishra P, Agrawal GP (2008) An insight on hyaluronic acid in drug targeting and drug delivery. J Drug Target 16:91–107

Yildiz I, McCaughan B, Cruickshank SF, Callan JF, Raymo FiM (2009) Biocompatible CdSe-ZnS core-shell quantum dots coated with hydrophilic polythiols. Langmuir 25:7090–7096

Yildiz I, Deniz E, McCaughan B, Cruickshank SF, Callan JF, Raymo FiM (2010) Hydrophilic CdSe-ZnS core-shell quantum dots with reactive functional groups on their surface. Langmuir 26:11503–11511

Ying JY, Zarur A (2002) Synthesis of nanometer-sized particles by reverse micelle mediated techniques. US Patent 6,413,489

Zhang P et al (2012) Click-functionalized compact quantum dots protected by multidentate-imidazole ligands: conjugation-ready nanotags for living-virus labeling and imaging. J Am Chem Soc 134:8388–8391

Zheng H, Chen G, DeLouise LA, Lou Z (2010) Detection of the cancer marker CD146 expression in melanoma cells with semiconductor quantum dot label. J Biomed Nanotechnol 6:303–311